

# Cortical Layer-dependent Basal CBV and stimulation-induced CBV Responses

F. Zhao<sup>1,2</sup>, P. Wang<sup>1,2</sup>, K. Ugurbil<sup>2</sup>, S-G. Kim<sup>1,2</sup>

<sup>1</sup>Neurobiology Department, Brain Imaging Research Center, Pittsburgh, PA, United States, <sup>2</sup>Center for Magnetic Resonance Research, Minneapolis, MN, United States

## ABSTRACT

To examine cortical layer-dependent basal CBV and stimulation-induced CBV responses, the cat visual stimulation model was used at 9.4T. Baseline total-CBV and microvascular-CBV were obtained by measuring  $R_2^*$  and  $R_2$  changes induced by 10 mg/kg MION. The highest total CBV is located at the CSF area containing large pial vessels, while the highest microvascular CBV is located at the middle of the cortex. GE and SE fMRI were obtained after the injection of MION. The maximal signal changes are occurred at the middle cortical layers, suggesting that the CBV response can be used to detect layer-dependent fMRI signal changes.

## INTRODUCTION

Signal change induced by blood-pool contrast agents (MION) is sensitive to local vascular density and vessel size (1). Thus, change in  $R_2$  and  $R_2^*$  induced by contrast agents is directly related to microvascular and total blood volumes, respectively (1). Similarly, CBV-weighted fMRI signal change is dependent on a change in CBV induced by neural activity and the basal CBV. For examining laminar-dependent baseline CBV and neural activity-induced CBV responses, we obtained high-resolution SE and GE fMRI in the cat visual cortex after the injection of MION during visual stimulation.

## METHODS

Cats ( $n = 5$ ) were intubated and maintained under  $\sim 1.3\%$  isoflurane. End-tidal  $CO_2$  (3.0-3.8%) and temperature were maintained under a normal condition (2). The binocular visual stimuli consisted of drifting square-wave gratings (0.15 cycle/degree, 2 cycles/s). All NMR measurements were performed on a 9.4T/31cm MRI system (Magnex/Varian) with a 1.6-cm diameter surface coil. Coronal images with 128x128 matrix size and FOV of  $2 \times 2 \text{ cm}^2$  were obtained using the 4-segmented EPI technique with navigator echo. Baseline  $R_2$  and  $R_2^*$  maps were obtained before and after the injection of 10 mg/kg MION. fMRI was obtained after the injection of MION. For GE fMRI, TE = 10 ms, TR = 1 s, and effective TR = 4.0 s. For SE fMRI, the double SE EPI sequence with adiabatic pulses (3) was used. The SE fMRI parameters were: TE = 25 ms, TR of each segment = 2 s, and effective TR = 8 s. To obtain comparable CNRs in GE and SE fMRI, SE fMRI experiments were obtained at 3 times more than GE experiments in an interleaved manner. After averaged all experiments, cross correlation (CC) values were calculated with a boxcar reference function. Percent signal change induced by visual stimulation was calculated where a pixel had CC  $\geq 0.3$  with the number of active cluster size  $\geq 4$  (Fig. 1 E and F). For depth-specific signal analysis (Fig. 2), two rectangular sections in area 18 (one at each hemisphere; green ROIs in Fig. 1A) within the visual cortex were selected, and pixels along lines perpendicular to the dorsal surface were determined without using any statistical threshold. To average signals at the same depth, pixels were spatially interpolated to 78  $\mu\text{m}$  nominal-resolution, then averaged signals across cortical layers were plotted as a function of distance from the surface of the cortex.

## RESULTS

Figure 1 shows one representative data set, consisting of  $T_1$ -weighted EPI image (A), baseline  $T_2$  (B),  $\Delta R_2^*$  and  $\Delta R_2$  induced by MION without any visual stimulation (C and D), and percent signal changes of SE and GE CBV-weighted fMRI during visual stimulation (E and F). Scale bars are 2 mm. Distance from the surface of the cortex to white matter is  $\sim 1.7$  mm. The CSF area containing the sagittal sinus (green contours in B) was selected because its  $T_2$  is longer than  $T_2$  of white and gray matter, and not included for depth-specific analysis. The largest total CBV (i.e., white area in C) was mainly located in the surface of the cortex, and intracortical vessels were often detected (C). However, the large microvascular CBV was located, not in the surface of the cortex, but in the middle of the cortex (D). In both CBV-weighted fMRI with SE (E) and GE (F) signal detection, the highest percent signal changes were observed at the middle of the cortex (color bar: 0.3-2% for E and 0.3-10% for F). Figure 2 shows profiles of  $\Delta R_2$  and  $\Delta R_2^*$  induced by MION without stimulation, and stimulation-induced CBV-weighted fMRI signals as a function of distance from the surface. The surface of the cortex is at zero. Basal  $\Delta R_2$  induced by MION ( $\Delta R_2$  MION; circles), related to basal microvascular CBV, is the highest at the middle layers of the cortex, while basal  $\Delta R_2^*$  induced by MION ( $\Delta R_2^*$  MION; squares) is the highest at the surface of cortex. During visual stimulation, the highest percent changes of SE (circles) and GE (squares) CBV-weighted fMRI were observed at the middle of the visual cortex,  $\sim 1.0$  mm from the surface, which is likely to be layer IV (4). The large change in the microvascular volume at the surface of the cortex was also observed, which may be due to  $T_2^*$  contribution of large vessels and/or actual microvascular signal change. Percent change in CBV-weighted fMRI is directly related to a change in absolute CBV and concentration of contrast agents in blood. Since concentration of MION in blood is constant, the percent change can be considered as an index of absolute CBV change. The point spread function of microvascular CBV response is narrower than that of total CBV response. All 5 animals' data are consistent. In order to determine accurate relative CBV changes, we need to consider the BOLD contribution to CBV-weighted fMRI, baseline CBV, and spatial blurring along phase-encoding (dorsal-ventral) direction during data acquisition. The most important finding is that the CBV response is not widespread, and can be used to detect layer-dependent fMRI signal changes.

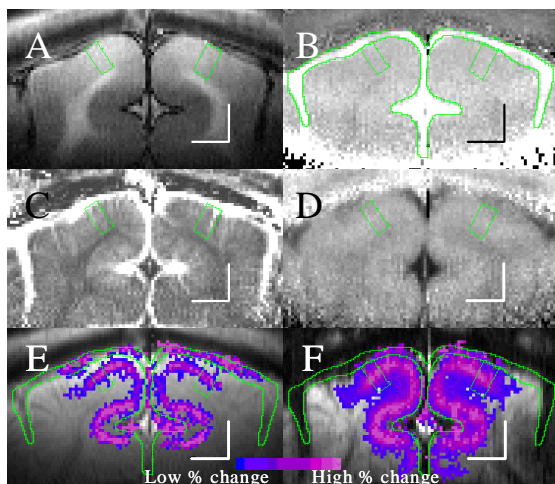


Fig. 1. SE and GE CBV-weighted fMRI

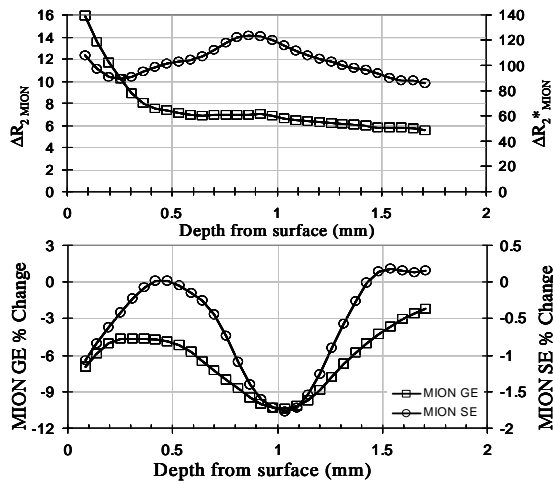


Fig. 2. Profiles of CBV and stimulation-induced CBV-weighted fMRI signal change.

## Reference

- (1) Boxerman JL, et al. MRM 1995 34:555-566.
- (2) Duong TQ, et al. MRM 2000; 44: 231-242.
- (3) Lee S-P, et al. MRM 1999; 42: 919-928.
- (4) Payne BR & Peters A. The Concept of Cat Primary Visual Cortex. Academic Press; 2002.

## Acknowledgement

(Supported by NIH (EB003375, EB003324, RR08079, RR17239) and McKnight Foundation)